Macromolecules

ARTICLE

pubs.acs.org/Macromolecules

Scrolled Polymer Single Crystals Driven by Unbalanced Surface Stresses: Rational Design and Experimental Evidence

Huiming Xiong,[†,‡] Chun-Ku Chen,[§] Kyungmin Lee,[†] Ryan M. Van Horn,[†] Zheng Liu,[∥] Bin Ren,[∥] Roderic P. Quirk,[†] Edwin L. Thomas,[⊥] Bernard Lotz,[#] Rong-Ming Ho,[*,§] Wen-Bin Zhang,[*,†] and Stephen Z. D. Cheng[*,†]

[†]Department of Polymer Science, College of Polymer Science and Polymer Engineering, University of Akron, Akron, Ohio 44325-3909, United States

[‡]Department of Polymer Science and Engineering, School of Chemistry and Chemical Engineering, Shanghai Jiao Tong University, Shanghai 200240, China

[§]Department of Chemical Engineering, National Tsing Hua University, Hsinchu 30013, Taiwan

[∥]State Key Laboratory of Physical Chemistry of Solid Surfaces, College of Chemistry and Chemical Engineering, Xiamen University, Xiamen 361005, China

[⊥]Department of Materials Science and Engineering, Massachusetts Institute and Technology, Cambridge, Massachusetts 02139, United States

[#]Institut Charles Sadron, 23, Rue du Loess, Strasbourg 67034, France

Supporting Information

ABSTRACT: To understand the formation mechanism of nonflat polymer single crystals, two types of triblock copolymers with a middle crystalline block and two amorphous, immiscible end-blocks were designed and synthesized. Specifically, polystyrene-*block*-poly(ethylene oxide)-*block*-poly(1-butene oxide) and polystyrene-*block*-poly(ethylene oxide)-*block*-polydimethylsiloxane were examined. When the end-blocks possess different volumes and are microphase separated onto the opposite sides of the single crystal lamella formed by the middle crystalline block, unbalanced surface stress can be generated. As a result, large scrolled single crystals (~80 μm) were grown from dilute solution using the self-seeding procedure at low supercoolings. The scrolling direction was identified to be along the (120) planes based on transmission electron microscopy (TEM) observations of the sedimented scrolled single crystals, which is in line with the fact that the scrolling occurs along the planes with the highest coefficient of thermal expansion. Using high-resolution TEM at high tilting angles, three layers of distinct chemical compositions can be clearly identified from the edges of the single crystals after RuO_4 staining. It suggests the formation of microphase separated domains of the amorphous end-blocks on the opposite sides of PEO single crystals. Although the tethering densities of these amorphous end-blocks are identical, their reduced tethering densities are different, resulting in dissimilar volumes and surface crowdedness on the opposite sides of PEO single crystal. The unbalanced surface stress is thus generated to scroll the lamellar single crystal. Macroscopically, based on the observed curvature and the assumption of a solid plate cylinder, the strain energy for each individual single crystal with lateral size of 80 μm was estimated to be $\sim 3 \times 10^{-9}$ erg, which, though small, is sufficient to maintain the scrolling of single crystal in solution at room temperature (the thermal energy is approximately $kT \sim 4 \times 10^{-14}$ erg). Microscopically, the difference of the reduced surface free energy of the tethered blocks at the opposite sides of the PEO lamellar single crystal is analyzed and understood to be the driving force of the scrolling.

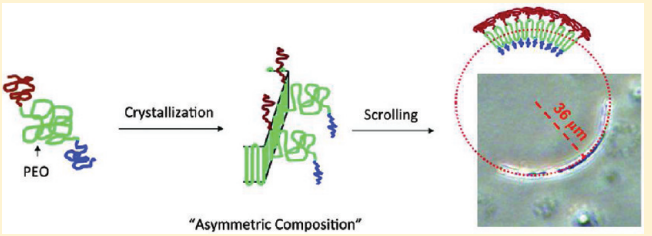

INTRODUCTION

Curved (or nonflat) lamellar crystals usually involve either twisting or scrolling. Ever since the discovery of polymer single crystals and the unveiling of the chain folding principle, they have been frequently observed.[1−5] For example, scrolled single crystals in solution were first reported in the early 1970s in various polymers including poly(4-methyl-1-pentene),[6] polychlorotrifluoroethylene,[7] and polyoxymethylene.[8] The curvature of the crystals was found to increase with decreasing crystallization temperature (T_x). Individual fold domains (sectors) in these cases were believed to be nonplanar as well. More recently, scrolled morphologies have also been found in the single crystals

Received: June 12, 2011
Revised: July 18, 2011
Published: September 12, 2011

of nylon-66,[9] isotactic poly-1-butene,[10] and chiral nonracemic *R*- and *S*-poly(epichlorohydrin) grown in solution.[11] The most striking and unexpected experimental observation was found in nylon-66 single crystals grown at T_x of 172 °C in gloslin after self-seeding at different temperatures (T_s).[12] With increasing T_s from 202 to 208 °C, the nylon-66 single crystals undergo a flat-to-scroll-to-flat transition. It should be noted that the lamellar thickness of the single crystals crystallized at a specific T_x is determined by the remaining seeds after the self-seeding process and their folded surfaces usually contain amide and/or acid folds with different number of carbon atoms (4 and 6, respectively), as determined by T_s. When the amide folds and acid folds are present on both sides of the lamellar crystals, they are flat. However, scrolling occurs when the two types of the folds are segregated onto the opposite surfaces of the lamellar crystal at specific lamellar crystal thicknesses.[12]

Nonflat polymer crystals have also been observed in the bulk. The γ-form crystalline lamellae of poly(vinylidene fluoride) (PVDF), which build up the spherulites, exhibits an intriguing, highly curved, "scroll-like" morphology with the scrolling axis parallel to the spherulite radius.[13] The scrolling is attributed to the imbalance of fold compositions, i.e., the presence of different numbers of $-CH_2-$ and $-CF_2-$ groups on the opposite fold surfaces due to steric constraints on the fold conformation. This is also reflected by the polarity of the γ-phase crystal structure.[14] Although cooperative lamellar twisting had been invoked in 1950s to explain the periodic banding (or concentric rings) observed in polyethylene (PE) spherulites under polarized optical microscope,[15−18] individual twisted lamellar crystals of PE were not observed until 1989 in the ultrahigh molecular weight polyethylene physical gels in decalin.[19] Twisted single lamellae were also observed in a series of nonracemic chiral polyesters with right- or left-handed chiral centers and different main chain paraffin groups.[20−27] The twist sense of the lamellae was found to depend not only on the handiness of the chiral center but also on the number of methylene units in the main chain.

Different mechanisms have been proposed to account for the origin and formation of curved lamellar crystals.[28−30] A simple manifestation of lamellar twisting and its mechanical origin were suggested by Keith and Padden to be the unbalanced surface stresses.[28,30] This mechanism unifies the origin of twisting and scrolling of the lamellar crystals, as commented by two of the authors recently.[29] With unbalanced surface stresses, the lamellae would either twist along a 2-fold axis parallel to the growth direction if such an axis exists or scroll otherwise. This model may not satisfactorily provide all of the necessary details to fully explain many different experimental observations, but it presents a way of thinking and analyzing toward understanding them. In this study, we aim to examine this model by utilizing two types of triblock copolymers, namely, polystyrene-*block*-poly(ethylene oxide)-*block*-poly(1-butene oxide) (PS-*b*-PEO-*b*-PBO) and polystyrene-*block*-poly(ethylene oxide)-*block*-polydimethylsiloxane (PS-*b*-PEO-*b*-PDMS), composed of a crystalline middle block and two amorphous, highly immiscible end-blocks (Scheme 1). The two end-blocks with different molecular weights (and, thus, volumes) are anticipated to be tethered on the opposite sides of the PEO single crystals upon crystallization. The asymmetric distribution of chemical compositions, or microphase separation, was confirmed by transmission electron microscopy (TEM) at high tilting angles. Although their tethering densities (σ) are identical, the difference in their reduced tethering densities ($\tilde{\sigma}$) on the crystalline substrates results in significant variation in surface crowdedness on the opposite sides of lamellar single crystal. In particular, at high $\tilde{\sigma}$ values above the onset of overcrowding ($\tilde{\sigma} \sim 3.7$),[31−33] the unbalanced surface stresses would be substantial to scroll the single crystals. This was indeed observed for both triblock polymers crystallized in dilute solution. Based on the observed curvature and the assumption of solid plate cylinder, the strain energy for each individual single crystal can be estimated and compared to other energy forms to shed light into the stability of the scrolled morphology.

Scheme 1. Illustration of the Crystallization of a Triblock Copolymer with a Crystalline Middle Block and Two Amorphous End-Blocks[a]

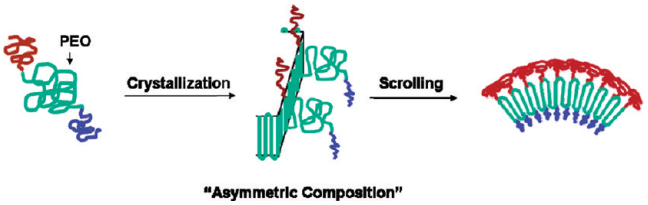

[a] The lamellar single crystal scrolls due to unbalanced surface stresses generated by the asymmetric compositions.

Table 1. Summary of Molecular Characterization, Lamellar Thicknesses, and Tethering Densities

	M_n (kg mol^{-1})	ρ (g cm^{-3})	v	d_{PEO} (nm)	σ (nm^{-2})	R_g (nm)	$\tilde{\sigma}$
PS-*b*-PEO-*b*-PBO (PDI = 1.03), d_0 = 16 nm at T_x = 37 °C							
PS	9.2	1.052	0.43		0.47	4.1	7.9
PEO	11.5	1.239	0.45	7.3			
PBO	2.3	0.952	0.12		0.47	1.4	1.0
PS-*b*-PEO-*b*-PDMS (PDI = 1.03), d_0 = 13 nm at T_x = 42 °C							
PS	5.7	1.052	0.32		0.46	3.1	4.4
PEO	11.4	1.239	0.54	7.0			
PDMS	2.3	0.96	0.14		0.46	1.3	0.8

EXPERIMENTAL SECTION

Materials. The PS-*b*-PEO-*b*-PBO triblock copolymer was synthesized via sequential anionic polymerization of styrene, ethylene oxide, and 1-butene oxide using high-vacuum techniques.[34] The synthesis of the polystyrene-*b*-poly(ethylene oxide)-*b*-polydimethylsiloxane (PS-*b*-PEO-*b*-PDMS) triblock copolymer follows a coupling strategy since it offers better control over the molecular weight and molecular weight distribution of the PDMS block. The detailed synthetic procedures can be found in the Supporting Information. The molecular characteristics of these triblock copolymers have been summarized in Table 1.

Instrumentation and Experiments. Phase contrast microscopy (PCM, Olympus BH-2) was used to observe the shape and morphology of the single crystals in solution or on glass substrate after the single crystals were sedimented and the solvent was evaporated.

Wide-angle X-ray diffraction (WAXD) experiments were conducted on a Rigaku 12 kW rotating-anode X-ray generator with the wavelength at 0.1542 nm (Cu Kα) in the reflection mode. The X-ray beam was line-focused and monochromatized using a graphite crystal. The beam size was controlled by a series of slits with a divergence slit of 0.5°, a receiving slit of 0.15 mm, and a scattering slit of 0.5°. The diffraction peak *d*-spacings were calibrated with silicon crystals of known crystal lattice in the high 2θ-angle region (>15°) and silver behenate in the low 2θ-angle

dx.doi.org/10.1021/ma201325t |*Macromolecules* 2011, 44, 7758–7766

region (<15°). The 2θ angular resolution in WAXD experiment was within ±0.05°. A hot stage was coupled to the diffractometer in order to obtain the coefficients of thermal expansion (CTE) of PEO crystals of different crystalline planes by monitoring the *d*-spacing changes with temperatures during heating. The temperature of the hot stage was calibrated by the standards with known melting temperatures.

The overall single crystal lamellar thicknesses were measured by atomic force microscopy (AFM, Digital Instruments Nanoscope IIIA) under the tapping mode. The cantilever force was properly selected to make sure that it was light enough to avoid any damage to the sample and strong enough so that the surface features could be accurately explored. The scanning rate was 1 Hz for low-magnification images at a resolution of 512 × 512 pixels per image.

Experiments of TEM were performed with a JEOL JEM-2100 LaB_6 transmission electron microscopy at an accelerating voltage of 200 kV. The bright-field (BF) images were obtained using the mass thickness contrast imaging. To obtain the TEM image series with alignment, proper amounts of fiducial gold markers (Polysciences, $d \sim 10$ nm) need to be spread over the samples uniformly so that the grain boundaries can be observed for tilting experiments. A series of 75 TEM images were collected from −74° to +74° tilt angles (the maximum tilting angles possible for the instrument) at an angular interval of 2°. Images were recorded on a Gatan CCD camera. Alignment of the tilt series was performed using IMOD software. In order to determine the crystal structures, selected area electron diffraction (SAED) experiments were also carried out in the TEM. The ED *d*-spacing was calibrated using the electron diffraction pattern of thallium chloride (TlCl) as a standard.

Sample Preparation. The self-seeding procedure was employed for single crystal growth in this study.[35−38] The single crystals of PS-*b*-PEO-*b*-PBO and PS-*b*-PEO-*b*-PDMS were grown in a mixed solvent of amyl acetate/*n*-octane (1:1 weight ratio). The dissolution temperature (T_d) was set at 70 °C. The self-seeding temperature (T_s) was around 54 °C. The crystallization temperature (T_x) varied from 35 to 42 °C. It usually required ∼10 h to complete the crystallization. Sometimes, especially at high T_xs, the crystallization may not be complete. Additional care must be taken to avoid overgrowth of the not-yet-crystallized polymers on the single crystals when the solution is cooled to room temperature for sample collection. After crystallization, the solution was usually filtered at T_x to collect the single crystals.

For phase contrast microscopy (PCM) observation in solution, the solution samples were dropped onto the glass slides with a built-in solution container. Single crystal mats were prepared by sedimentation of the single crystals for wide-angle X-ray diffraction (WAXD) experiments. The suspension of single crystals at the crystallization temperature was filtered under reduced pressure and washed with pure solvent at the same temperature before cooling to room temperature. The mats were then dried under vacuum. For atomic force microscopy (AFM) observation, a few drops of the single crystal suspension were placed onto carbon-coated cover glasses and washed with pure amyl acetate several times. The samples were then dried in a vacuum oven at room temperature to remove the residual solvent before AFM experiments to determine the morphology and lamellar thickness.

To prepare samples for transmission electron microscopy (TEM) experiments, a drop of the crystal suspension was deposited onto a copper grid (with 100 mesh) covered by a carbon-coated polyvinyl formal membrane, and the solvent was evaporated. Staining was accomplished by exposing the samples to the vapor of a 4% aqueous RuO_4 solution for 1 h. The RuO_4 preferentially attacks the double bonds in the PS blocks, rendering these microphase-separated domains dark in TEM via mass thickness contrast. The domains containing less or no PS will appear as gray and bright, respectively.

RESULTS AND DISCUSSION

Scrolled Single Crystals of Triblock Copolymers Grown in Solution. Both PS-*b*-PEO-*b*-PBO and PS-*b*-PEO-*b*-PDMS triblock copolymers were used to grow single crystals utilizing self-seeding technique for the PEO blocks. Figure 1 shows a set of PCM images for the PS-*b*-PEO-*b*-PBO (9.2k-11.5k-2.3k) single crystals grown in the mixed solvent of amyl acetate/*n*-octane (w/w = 1/1) at T_x = 37 °C in a time sequence of 5 min to take each image. Figure 2a shows the phase contrast images of PS-*b*-PEO-*b*-PDMS (5.7k-11.4k-2.3k) single crystals grown in the mixed solvent of amyl acetate/*n*-octane (w/w = 1/1) at T_x = 42 °C and observed in solution at room temperature. The squarelike single crystals were found to be indeed scrolled in both cases. As shown in Figure 1, the crystal slowly tumbles in solution and the scrolled shape is maintained throughout this period of time. The scrolled lamella possesses a radius of 36 μm with a curvature of 0.028 μm^{-1}. Hence, the splay angle between successive stems in PEO crystal lattice can be determined to be 0.0007°. This angle is too small to be detected by the lattice change using diffraction techniques. Nevertheless, the scrolling still exerts a compression on one surface of the lamella and an extension on the other so as to create strain energy within the crystal. Upon sedimentation, since the curvature of the single

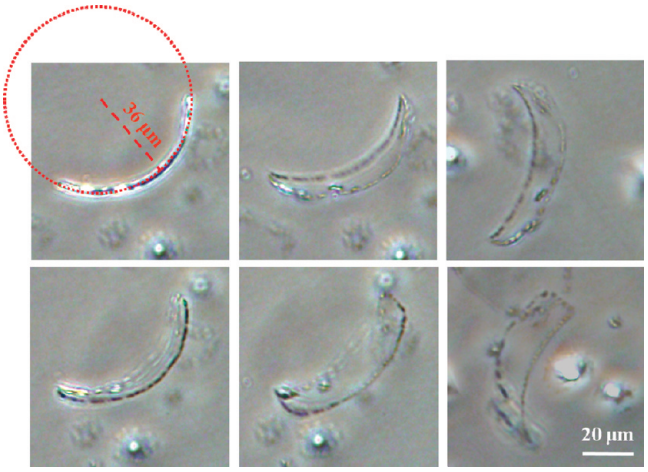

Figure 1. A series of PCM images for scrolled PS-*b*-PEO-*b*-PBO (9.2k-11.5k-2.3k) single crystals (T_x = 37 °C) in a mixed solvent of amyl acetate/*n*-octane (w/w = 1/1) at different times with a time interval of 5 min between taking images.

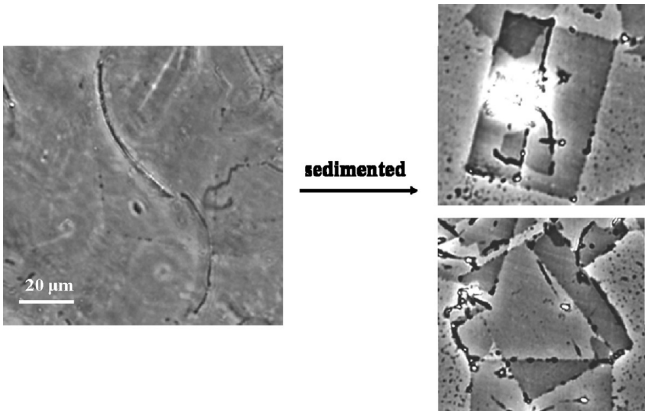

Figure 2. PCM images of scrolled PS-*b*-PEO-*b*-PDMS (5.7k-11.4k-2.3k) single crystals (T_x = 42 °C) in solution (left) and on glass substrate (right) after sedimentation.

crystals could not be solidly held, the single crystals either spread out to become flat with some buckles or collapse onto themselves to form folded, bilayered lamellae (Figure 2). As a result, the WAXD pattern of the precipitated single crystal mats remains identical to those of the homo-PEO's and the PS-*b*-PEO diblock copolymer's.[37−39]

The population of scrolled single crystals was found to be the majority at high T_x (low supercooling, ΔT) and slow crystal growth rates. When the ΔT became higher where crystal growth rates were faster, a decrease of the population of the scrolled single crystals was observed accompanied by an increase of the population of the flat lamellar crystals. However, further decreasing the T_x led to screwed single crystals, which complicates the identification of the crystals with or without scrolling. Formation of the scrolled single crystal is facilitated by decreasing growth rates where well-defined microphase separation of the end-blocks may occur on the opposite sides of the single crystals. It is noted that the scrolling curvature of the lamellar single crystals is not significantly affected by changing the ΔT in the low ΔT range studied. It was anticipated that the PEO crystal lamellar thickness and the stiffness of the crystals would be increased by decreasing the ΔT so as to result in a decrease of curvature. However, by comparing the results in Figures 1 and 2, the effect of molecular weight differences between two end-blocks seems to be much more profound than that of ΔT. Despite the higher T_x required to grow single crystals as demonstrated in Figure 2, the curvature of the single crystal in Figure 1 is apparently much larger than that in Figure 2. We attributed this effect to the significantly higher asymmetry introduced by molecular weight (and, thus, volume) difference, as reflected by the molecular weight ratio between PS and the other end-block (~4 for PS-*b*-PEO-*b*-PBO vs ~2.5 for PS-*b*-PEO-*b*-PDMS). It is also reasonable to suggest that the quality and selectivity of the solvent for the amorphous end-blocks may also affect the scrolling curvature due to the changes on the microphase separation and their reduced tethering densities, which are topics of future investigations.

After sedimentation, the overall thickness of the single crystal (d_0) can be measured by AFM.[33] Assuming an ideally phase-separated, three-layered structure of PS/PEO/PBO or PS/PEO/PDMS and identical density of each block to that in the bulk at 25 °C (ρ_{PS} = 1.052 g cm^{-3}, $\rho_{PEO,CRYST}$ = 1.239 g cm^{-3}, ρ_{PBO} = 0.952 g cm^{-3},[40] and ρ_{PDMS} = 0.965 g cm^{-3}), the thickness of the PEO lamellar single crystals (d_{PEO}) can be estimated from the volume fraction of the PEO using the following equations:[33,41]

$$d_{PEO} = d_0 v_{PEO} \quad (1)$$

$$v_{PEO} = \frac{M_n^{PEO}/\rho_{PEO}}{M_n^{PS}/\rho_{PS} + M_n^{PEO}/\rho_{PEO} + M_n^{PBO}/\rho_{PBO}} \quad (2)$$

where v_{PEO} is the volume fraction of PEO crystalline block and M_n is the molecular weight of each block. The tethering density (σ) can then be calculated from the lamellar thickness using the following equations:

$$\sigma = 1/S \quad (3)$$

$$S = \frac{M_n^{PEO}}{N_A \rho_{PEO} d_{PEO}} \quad (4)$$

where S is the average area covered by each polymer chain and N_A is Avogadro's number. Unlike diblock copolymer systems as described in eq 2 of ref 33, there is not a factor of 2. Although every lamellar single crystal has two folded surfaces, each triblock copolymer chain provides two tethered block chains to cover these surfaces. As a result, the factor of 2 should be canceled out, yet the tethering densities for each block are still identical in this case. The results are summarized in Table 1. Specific attention should be paid to the d_{PEO} values in Table 1 which are 7.3 and 7 nm, respectively. Compared with our previous studies,[31−33] these values are small. The reason for the small d_{PEO} values is due to the fact that the mixed solvent of amyl acetate and *n*-octane that we used in this study is much poorer, and thus, the dissolution and self-seeding temperatures in this study are much higher than those in our previous study.[31−33]

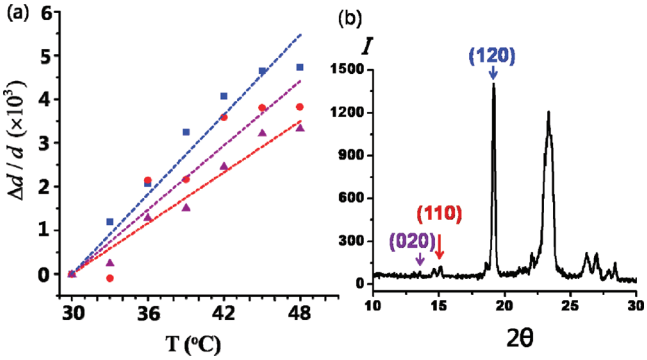

Figure 3. (a) Temperature dependences of the relative *d*-spacing changes of (120), (110), and (020) planes for the single crystal mats of PS-*b*-PEO: blue square, (120); red circle, (110); purple triangle, (020) diffractions. (b) A typical 1D WAXD pattern of PEO lattice showing the peaks that can be assigned to (020), (110), and (120), respectively.

Scrolling Direction of Triblock Copolymer Single Crystals. The scrolling direction could be deduced either from the image of the crystals in solution or the reconstructed single crystal morphologies after sedimentation. As shown in Figure 1, it is very likely that the single crystal is scrolled along the edge. When these scrolled single crystals are transferred onto a substrate, the collapse of the single crystals usually occurs along the scrolling direction (Figure 2). The reconstruction of such collapsed single crystals also suggests that the folding direction is more or less along the edge which is the (120) plane. As a result, it is reasonable to suggest that the (120) lattice should be the easiest one to deform via bending, expanding, or compressing. This can be probed by measuring and comparing the coefficients of thermal expansion (CTEs) of the lattice along the different crystalline planes. It is known that the largest CTE should be from the crystalline planes with the weakest stiffness/modulus. Hence, it provides an indirect evidence to identify the scrolling direction of the single crystals. Temperature-resolved WAXD experiments on single crystal mats of PS-*b*-PEO (9k-11k)[38] were conducted as a model system to identify different CTEs along the various crystalline planes of the PEO single crystals and to elucidate our prediction of the most probable scrolling direction for the PEO single crystals.

Figure 3a shows the relative changes in the lattice *d*-spacings ($\Delta d_{(hkl)}/d_{(hkl)}$) of the (120), (100), and (020) planes at a temperature T with respect to that at 30 °C, and Figure 3b shows a typical 1D WAXD pattern and corresponding diffraction assignments. The CTEs, $(\Delta d_{(hkl)}/d_{(hkl)})/\Delta T$, in the temperature range studied can be determined from the slopes of the plots in Figure 3a by a linear regression as the first approximation. Compared to the

dx.doi.org/10.1021/ma201325t |*Macromolecules* 2011, 44, 7758–7766

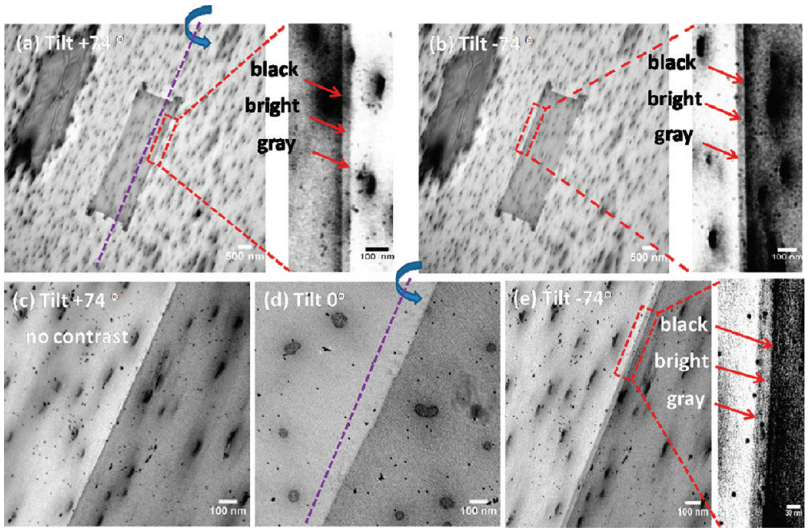

Figure 4. TEM bright field projection images of the single crystal at tilting angles of +74° (a) and −74° (b) and a series of projection images focusing on the left edge of the PS-*b*-PEO-*b*-PDMS (5.7k-11.4k-2.3k) at tilting angles of +74° (c), 0° (d), and −74° (e). The insets in (a), (b), and (e) are the enlarged images of the corresponding single crystal edges to show the trilayered contrast. The purple dashed line is the tilting axis.

CTEs of the (020) and (110) planes [$(2.5 \pm 0.2) \times 10^{-4}$ and $(1.9 \pm 0.1) \times 10^{-4}$ °C^{-1}, respectively], the CTE of the (120) planes [$(3.0 \pm 0.2) \times 10^{-4}$ °C^{-1}] was found to be the largest. Hence, the direction along the (120) planes should be the easiest to deform. This is an indirect evidence to demonstrate that the direction along the (120) plane is the most probable direction for scrolling.

Bar twining, PEO single crystals are square-shaped under this crystallization condition.[31−33,35−38] Based on the results of 1D WAXD techniques, the direction along the (120) plane seems to be the most probable scrolling direction. A further question then arises with respect to the scrolling direction: why do the single crystals prefer to scroll along one set of (120) planes instead of bending simultaneously along two orthogonal sets of the (120) planes to form a bowl-like crystal morphology? The answer should thus be relevant to the comparison between the 1D deformation free energy in forming the scrolled crystal and the 2D deformation free energy in forming the bowl-like crystal. A perfect square habit itself does not have any preference along which set of the (120) planes to scroll. However, as soon as the 1D deformation initiates along one set of the (120) planes to scroll, it prevents the deformation along the orthogonal set of the (120) planes. The reason is due to the fact that the 1D deformation only introduces a crystal lattice strain along one direction, while the 2D deformation along the orthogonally scrolling directions require a much severe crystal lattice strain along two directions. The crystal growth under this 2D deformation condition is much less favorable (with its higher barrier) than that under the 1D deformation condition. Therefore, the 2D deformation along the orthogonally scrolling directions results in a greater penalty of the free energy and destabilizes the single crystal. As a result, the single crystal can only scroll along one set of the (120) planes to release the unbalanced surface stresses instead of developing a second scrolling along the orthogonal direction to form the bowl-like single crystal morphology.

Identification of Asymmetric Distribution of Chemical Compositions. Although the origin of the scrolled single crystals remains an open question, the mechanism of unbalanced surface stresses suggested by Keith and Padden is currently the most reasonable explanation for experimental observations. The unbalanced surface stresses are attributed to the asymmetric distribution of amorphous end-blocks with different volumes and compositions on the opposite sides of the lamella in these triblock copolymer single crystals. However, because the surface layer only possesses a thickness of ~3 nm out of the total lamellar thickness of ~14 nm, it is not easy to detect solely the chemical composition of the surface layer without interference from the center lamella and the opposite side, not to mention "distinguishing" them.[42] Moreover, the phase separation in reality might not be as perfect as expected. The degree of phase separation would be strongly dependent upon the crystal growth conditions. Only with slow crystal growth rates, a PS-rich surface layer and a PDMS-rich surface layer on the opposite sides of each PEO single crystal lamella may result. It is thus critical to clearly identify the difference in chemical compositions between the opposite sides of PEO single crystals in these triblock copolymer single crystals, such as PS-*b*-PEO-*b*-PDMS. Although various experimental methods were tried in vain, a method to look at the projection of the edges of the single crystal under TEM at high tilting angles finally provides a qualitative evidence to solve the problem.

Before TEM observation, the samples were stained with RuO_4. RuO_4 is known to preferentially stain PS segment so that the PS domains appear dark after staining. By contrast, the PDMS domains naturally appear gray because of the higher electron density of Si in the block backbones. For PEO single crystal lamella, it appears bright because of its higher density and less tendency for staining. Figure 4 shows the actual TEM bright field images of a RuO_4-stained PS-*b*-PEO-*b*-PDMS single crystal at different tilting angles. The insets in Figures 4a, 4b, and 4e are the enlarged images of corresponding single crystal edges at high tilting angles. To acquire explicit results at high tilting angles, small single crystals with lateral sizes of less than 5 μm were collected to conduct the experiments. In these small single crystals, the scrolling was not significant and the curvature was not solidly held. When they are deposited on the surface, they are spread out to become flat without buckling or collapsing. To

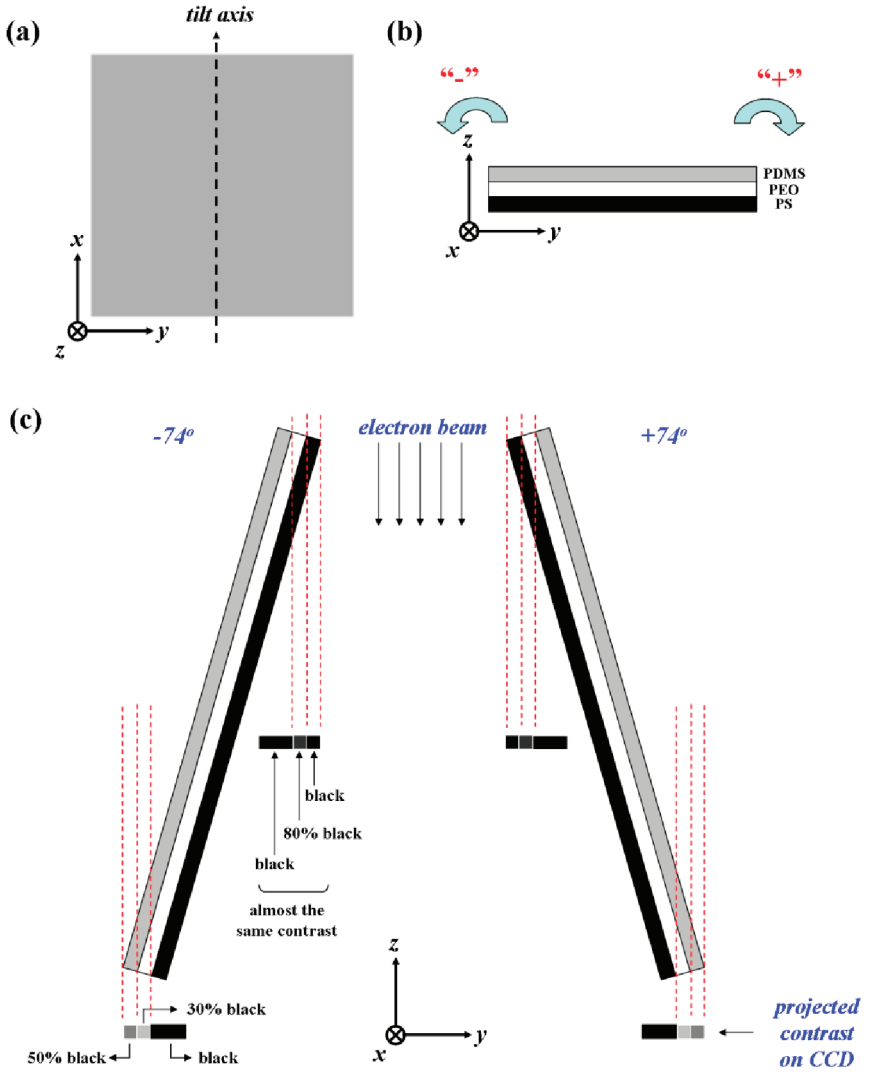

Figure 5. Simulation of projected contrast under TEM observation in which the PS layer of the single crystal is in contact with substrate. (a) The top and (b) side view of the three-layered structure of the single crystal. (c) Simulation of the change of projected contrast under TEM observation. The three-layered contrast can be observed at left and right edges as the tilting angles are −74° and +74°, respectively.

achieve better image alignment, gold fiducial markers were purposely addressed onto the surface of the crystals; they appear as small isolated black spots. Twenty gold markers were selected and tracked over the 75 images under projection at tilting angles between −74° and +74° (one image for every 2° tilting) to perform the image alignment by the least-squares method. From the aligned TEM images, the contrasts among different domains can be clearly identified once the tilting angle is higher than 65°. Figure 4a shows the TEM bright field image of the entire crystal taken at +74° tilting angle. The enlarged image in the inset reveals a three-layered structure at the right edge of the single crystals in the sequence of gray, bright, and dark on the substrate. It is noted that the "bright" layer is actually brightly gray due to the fact that PEO blocks can be slightly stained even in the crystalline state and/or some of the PDMS and PS blocks may lie down to cover part of the lateral crystal surface.[32] In comparison, the left edge of the single crystal appears completely dark with no discernible contrast. When the sample is tilted to −74° tilt angle (Figure 4b), the left edge of the single crystal shows up in the gray, bright, and dark contrast in sequence (see, the inset in Figure 4b) while the right edge is now completely dark with no contrast in imaging. Also, high-magnification TEM images were taken on the left edge of the single crystal at the tilting angles of +74°, 0°, and −74° (Figures 4c, 4d, and 4e, respectively), which further confirms the existence of different chemical compositions on the opposite side of the single crystal surface.

The interpretation of these TEM observations is illustrated in Figure 5. Since the phase separation in reality cannot be perfect, a PS-rich surface layer and a PDMS-rich surface layer might be formed on the opposite sides of the PEO single crystal lamella. On the assumption that the PS-rich layer is at the bottom, Figures 5a and 5b exhibit the top and side views of the PS-*b*-PEO-*b*-PDMS single crystal lamella, respectively. The color denotation is in accordance with the contrast due to RuO_4 staining. Since the TEM observation was made under the transmission mode, the difference in projection contrast could only be observed at the edges at high tilting angles (Figure 5c). In this way, the formation of three-layered structure and the relative arrangement of three layers can be simulated. For example, at −74° tilting angle, only the left edge exhibits a contrast of gray, bright,

dx.doi.org/10.1021/ma201325t |*Macromolecules* 2011, 44, 7758–7766

and dark in sequence. There is no discernible contrast at the right edge. In comparison, at +74° tilting angle, only the right edge exhibits a contrast of dark, bright, and gray in sequence. No contrast at the left edge could be recognized. The analysis is in line with the observations in Figure 4, confirming that the PS-*b*-PEO-*b*-PDMS crystal lamella is intrinsically a three-layered structure with a PS-rich layer at the bottom and a PDMS-rich layer on the top.

Since there is no specific interaction between the single crystal and the substrate, the deposition should occur randomly without any preference of which surface layer in contact with the substrate. Hence, there should also be single crystals with the PDMS-rich layer at the bottom and PS-rich layer on the top of the PEO single crystal lamella. From a similar simulation and analysis (Figure S8), we predict that the contrast in this case could only be observed on the right edge at the tilting angle of −74° in the dark, bright, and gray sequence or on the left edge at the tilting angle of +74° in the gray, bright, and dark sequence. Indeed, such single crystals were also observed (Figure S9), which is just the opposite of that in Figure 4. Therefore, using TEM projection imaging at high tilting angles, the differences in chemical compositions can be qualitatively distinguished between the opposite sides of the single crystal lamella.

Unbalanced Surface Stresses in Scrolled Triblock Copolymer Single Crystals. In the previous section, the scrolled single crystals were shown, and the asymmetric distribution of chemical compositions on the opposite sides of the single crystal was demonstrated. To the best of our knowledge, these are the first triblock copolymer single crystals grown in a scrolled form in solution. The rationale in this study is to create unbalanced surface stresses via the asymmetric distribution of chemical compositions on the opposite basal surfaces as the driving force for scrolling. It can be understood based on the analysis of the macroscopic strain energy and the microscopic free energy change associated with the scrolling. For the two amorphous end-blocks tethered on the opposite sides of the single crystal lamella, their tethering densities (σ) are identical, but their reduced tethering densities ($\tilde{\sigma}$) are significantly different due to different molecular weights and, thus, different radii of gyration in specific solvents (Table 1), which generates different surface crowdedness and thus unbalanced surface stresses on each side of the single crystal. The unbalanced surface stresses are, hence, of entropic origin.

The determination of PEO lamellar single crystal thickness (d_{PEO}) and the tethering density of the amorphous blocks have been described. Since the growth of single crystals was performed in a good solvent for the amorphous blocks (PS, PBO, and PDMS), their radii of gyration can be estimated on the basis of literature values and their reduced tethering densities can then be determined accordingly.[42] For PS-*b*-PEO-*b*-PBO, the σ value for both the PS and PBO blocks is 0.47 nm^{-2}. By assuming that the radius of gyration of the PS and PBO blocks in amyl acetate/octane is ∼4.1 nm for the PS with molecular weight of 9.2 kg mol^{-1} [42] and 1.4 nm for the PBO with molecular weight of 2.3 kg mol^{-1},[43] respectively, their $\tilde{\sigma}$ values were thus calculated to be 7.9 and 1.0, respectively. Similarly, for PS-*b*-PEO-*b*-PDMS, the σ values for the PS and PDMS blocks are both 0.46 nm^{-2}. By assuming that the radius of gyration of the amorphous blocks in amyl acetate/*n*-octane is roughly 3.1 nm for the PS with molecular weight of 5.7 kg mol^{-1} [42] and 1.3 nm for the PDMS with molecular weight of 2.3 kg mol^{-1},[44] their $\tilde{\sigma}$ values were calculated as 4.4 and 0.8, respectively. Significant differences between the reduced tethering densities are evident in both cases. Moreover, the reduced tethering density for the PS blocks in both cases is larger than 3.7, suggesting that a surface overcrowding should occur.[31,33] Therefore, it might be the main reason for the unbalanced surface stress which eventually leads to the scrolling of single crystals.

Semiquantitatively, let us now assume an ideal case as a first approximation in which the PS and PDMS (or PBO) blocks are completely segregated and tethered onto the two opposite sides of the single crystal lamellar surface. As a reference, we first consider the PS blocks which possess the same molecular weight and tethering density as in the triblock copolymer tethered on a flat PEO single crystal surface as a substrate. Similarly, we also consider the PDMS (or PBO) blocks which possess the same molecular weight and tethering density as in the triblock copolymer tethered on a flat PEO single crystal surface as a substrate. The reduced surface free energies for both cases can then be estimated based on our previous work.[33] For both the PDMS and PBO blocks, their reduced tethering densities are less than 3.7, and thus, both of their reduced surface free energies are zero. On the other hand, the reduced tethering densities of PS blocks are 4.4 for PS-*b*-PEO-*b*-PDMS and 7.9 for PS-*b*-PEO-*b*-PBO. Their corresponding reduced surface free energies are thus 1.9 and 2.6, respectively. The difference between the reduced surface free energies of PS and PDMS (or PBO) are thus the driving forces of the scrolling. Upon scrolling of the scrolled single crystal lamella, the side with the higher reduced surface energy (the PS block side) will experience expanding to decrease the reduced surface energy with increasing curvature. Oppositely, the side with the lower reduced surface energy (the PDMS or PBO block side) will experience compression and the reduced surface energy tends to increase with increasing curvature. At a specific curvature, the overall reduced surface energy reaches the minimum, which is the curvature observed in our experiments.

Alternatively, the scrolling of the single crystal can be used as a probe to identify the unbalanced surface stress and the associated strain energy in the system. According to the curvature, the strain energy per unit area can be estimated at mechanical equilibrium and related to the unbalanced surface stresses caused by the variation in reduced tethered densities on opposite fold surfaces. Under the assumption of a cylindrical rigid plate as a simple approximation, the strain energy per unit area can be calculated using eq 5:[43]

$$W = \frac{1}{24} E d^3 \left(\frac{1}{R_1} - \frac{1}{R_2} \right)^2 \quad (5)$$

where W is the strain energy per unit area, E is the modulus, d is the thickness of single crystal lamella, and $1/R_1$ and $1/R_2$ are the curvatures of the scrolled and flat morphologies, respectively. The (120) lattice modulus of PEO (E) is about 4.4 GPa according to the literature.[45] The thickness of the single crystal lamella (d) is about 7 nm, and R_1 equals 36 μm while $1/R_2$ is 0 in the case of PS-*b*-PEO-*b*-PBO. The strain energy per unit area can thus be estimated to be $\sim 5 \times 10^{-5}$ erg cm^{-2}. Hence, for a square-shaped PEO single crystal of 80 μm in lateral size, the total strain energy is $\sim 3 \times 10^{-9}$ erg, which is close to the estimation of deformed PE lamella with an S-bending to a radius of 1 μm ($\sim 5 \times 10^{-9}$ erg).[43] This is certainly a rough estimation, since (i) it is quite blunt to assume that the PEO single crystal is a rigid and isotropic plate and (ii) the modulus in crystals is in fact a fourth-rank tensor.[46] Nevertheless, it provides a qualitative

analysis of the strain energy in scrolled single crystals in comparison to other energy forms. For example, at room temperature, the strain energy of $\sim 3 \times 10^{-9}$ erg is 5 orders of magnitude larger than the thermal energy (approximately kT, $\sim 4 \times 10^{-14}$ erg). Thus, the single crystal can maintain its scrolled form in solution, as we observed in experiments (Figures 1 and 2). The strain energy can also be expressed in terms of J/mol. Consider the area of S with PEO lamellae thickness of d, the mole number of monomers (n) in this volume is

$$n = Sd\rho_{PEO}/M_0 \quad (6)$$

where ρ_{PEO} is the density of PEO crystal and M_0 is the molecular weight of the monomer. Because the strain energy (w) stored in this volume is $w = W \times S$, the strain energy per mole of monomer (H) could then be calculated using the following equation:

$$H = \frac{w}{n} = \frac{WS}{Sd\rho} M_0 = \frac{W}{d\rho} M_0 \quad (7)$$

The result is 2.5×10^{-4} J/mol, which is very small as compared to the heat of fusion of PEO (8.66 kJ/mol).[47] It means that the strain energy would not cause major phase disruption of the PEO single crystals, but only minor morphological deformation such as scrolling. Therefore, the macroscopic estimation of strain energy and microscopic analysis of the reduced surface free energy change provide insights into its origin on the molecular basis, the stability of the scrolled single crystals relative to thermal fluctuation, and the effects on the morphology and structure of the crystals.

CONCLUSIONS

In summary, two types of triblock copolymers, PS-*b*-PEO-*b*-PBO and PS-*b*-PEO-*b*-PDMS, with a middle crystalline PEO block and two amorphous, immiscible end-blocks have been designed and synthesized. Their lamellar single crystals were grown in dilute solutions using self-seeding techniques and found to be scrolled in solutions. To the best of our knowledge, this is the first time that scrolled single crystals are rationally designed and grown in solution in triblock copolymers. The origin of scrolling in these single crystals was attributed to the microphase separation of the two amorphous, immiscible end-blocks onto the opposite sides of the lamella. The resulting asymmetric distribution of chemical compositions was proven by high-resolution TEM experiments at high tilting angles. This generates different surface crowdedness and, thus, unbalanced surface stresses at the opposite sides of the single crystals, leading to the scrolling of the single crystals. Therefore, these unbalanced surface stresses are entropic in origin. The scrolling direction was identified to be most probably along the (120) plane by the PCM and TEM images both in solution and in collapsed single crystals, which was supported by the measurement of the CTEs along different crystalline planes. The curvature of the scrolled single crystal was used as a probe of the unbalanced surface stresses. Macroscopically, the strain energy for an entire single crystal 80 μm in size was estimated to be $\sim 3 \times 10^{-9}$ erg based on a simple approximation by assuming that the scrolled single crystal is a rigid and isotropic plate. Microscopically, the difference of the reduced surface free energy of the tethered blocks at the opposite sides of the PEO lamellar single crystal is analyzed and understood to be the driving force of the scrolling. Future research will be directed to investigate other factors that might affect the curvature of the scrolled single crystals, including molecular weight, asymmetric composition, crystal growth conditions, and the environment.

ASSOCIATED CONTENT

Supporting Information. Synthesis and characterization of PS-*b*-PEO-*b*-PBO and PS-*b*-PEO-*b*-PDMS; detailed explanation for the interpretation of TEM results. This material is available free of charge via the Internet at http://pubs.acs.org.

AUTHOR INFORMATION

Corresponding Author

*Tel + 1 330-972-6931, Fax + 1 330-972-8626, e-mail scheng@uakron.edu (S.Z.D.C.); Tel + 886-3-5738349, Fax + 886-3-5715408, e-mail rmho@mx.nthu.edu.tw (R.-M.H.); Tel + 1 330-990-9801, Fax + 1 330-972-8626, e-mail wz8@uakron.edu (W.-B.Z.).

ACKNOWLEDGMENT

This work was supported by NSF (DMR-0516602 and DMR-0906898).

REFERENCES

(1) Jaccodine, R. *Nature* **1955**, *176*, 305.
(2) Keller, A. *Philos. Mag.* **1957**, *2*, 1171.
(3) Till, J. P. H. *J. Polym. Sci.* **1957**, *24*, 301.
(4) Fischer, E. W. *Z. Naturforsch.* **1957**, *12*, 753.
(5) Nakajima, A. T. H., Tsuruta, T., Yuki, H., Ohtsu, T., Eds. *Kobunshi no Bussei (Properties of Polymers)*; Kagakudojin: Kyoto, 1962; Chapter 11.
(6) Khoury, F.; Barnes, J. D. *J. Res. Natl. Bur. Stand., Sect. A* **1972**, *76A*, 225.
(7) Khoury, F.; Barnes, J. D. *J. Res. Natl. Bur. Stand., Sect. A* **1974**, *78A*, 363.
(8) Khoury, F.; Barnes, J. D. *J. Res. Natl. Bur. Stand., Sect. A* **1974**, *78A*, 95.
(9) Geil, P. H. *J. Polym. Sci.* **1960**, *44*, 449.
(10) Holland, V. F.; Miller, R. L. *J. Appl. Phys.* **1964**, *35*, 3241.
(11) Saracovan, I.; Cox, J. K.; Revol, J. F.; Manley, R. S. J.; Brown, G. R. *Macromolecules* **1999**, *32*, 717.
(12) Cai, W. W.; Li, C. Y.; Li, L. Y.; Lotz, B.; Keating, M. N.; Marks, D. *Adv. Mater.* **2004**, *16*, 600.
(13) Vaughan, A. S. *J. Mater. Sci.* **1993**, *28*, 1805.
(14) Lotz, B.; Thierry, A.; Schneider, S. *C. R. Acad. Sci., Ser. IIc: Chim.* **1998**, *1*, 609.
(15) Point, J. *J. Bull. Acad. R. Bel.* **1953**, *41*, 982.
(16) Keith, H. D.; Padden, F. J., Jr. *J. Polym. Sci.* **1959**, *39*, 123.
(17) Keller, A. *J. Polym. Sci.* **1959**, *39*, 151.
(18) Price, F. P. *J. Polym. Sci.* **1959**, *39*, 139.
(19) Kunz, M.; Drechsler, M.; Moller, M. *Polymer* **1995**, *36*, 1331.
(20) Li, C. Y.; Yan, D. H.; Cheng, S. Z. D.; Bai, F.; He, T. B.; Chien, L. C.; Harris, F. W.; Lotz, B. *Macromolecules* **1999**, *32*, 524.
(21) Li, C. Y.; Cheng, S. Z. D.; Ge, J. J.; Bai, F.; Zhang, J. Z.; Mann, I. K.; Harris, F. W.; Chien, L. C.; Yan, D. H.; He, T. B.; Lotz, B. *Phys. Rev. Lett.* **1999**, *83*, 4558.
(22) Li, C. Y.; Cheng, S. Z. D.; Ge, J. J.; Bai, F.; Zhang, J. Z.; Mann, I. K.; Chien, L. C.; Harris, F. W.; Lotz, B. *J. Am. Chem. Soc.* **2000**, *122*, 72.
(23) Li, C. Y.; Cheng, S. Z. D.; Weng, X.; Ge, J. J.; Bai, F.; Zhang, J. Z.; Calhoun, B. H.; Harris, F. W.; Chien, L. C.; Lotz, B. *J. Am. Chem. Soc.* **2001**, *123*, 2462.
(24) Li, C. Y.; Ge, J. J.; Bai, F.; Calhoun, B. H.; Harris, F. W.; Cheng, S. Z. D.; Chien, L. C.; Lotz, B.; Keith, H. D. *Macromolecules* **2001**, *34*, 3634.

(25) Li, C. Y.; Jin, S.; Weng, X.; Ge, J. J.; Zhang, D.; Bai, F.; Harris, F. W.; Cheng, S. Z. D.; Yan, D. H.; He, T. B.; Lotz, B.; Chien, L. C. *Macromolecules* **2002**, *35*, 5475.
(26) Weng, X.; Li, C. Y.; Jin, S.; Zhang, D.; Zhang, J. Z.; Bai, F.; Harris, F. W.; Cheng, S. Z. D. *Macromolecules* **2002**, *35*, 9678.
(27) Jin, S.; Jeong, K. U.; Tu, Y.; Graham, M. J.; Wang, J.; Harris, F. W.; Cheng, S. Z. D. *Macromolecules* **2007**, *40*, 5450.
(28) Keith, H. D.; Padden, F. J. *Polymer* **1984**, *25*, 28.
(29) Lotz, B.; Cheng, S. Z. D. *Polymer* **2005**, *46*, 577.
(30) Keith, H. D.; Padden, F. J. *Macromolecules* **1996**, *29*, 7776.
(31) Chen, W. Y.; Zheng, J. X.; Cheng, S. Z. D.; Li, C. Y.; Huang, P.; Zhu, L.; Xiong, H. M.; Ge, Q.; Guo, Y.; Quirk, R. P.; Lotz, B.; Deng, L. F.; Wu, C.; Thomas, E. L. *Phys. Rev. Lett.* **2004**, 93.
(32) Chen, W. Y.; Li, C. Y.; Zheng, J. X.; Huang, P.; Zhu, L.; Ge, Q.; Quirk, R. P.; Lotz, B.; Deng, L. F.; Wu, C.; Thomas, E. L.; Cheng, S. Z. D. *Macromolecules* **2004**, *37*, 5292.
(33) Zheng, J. X.; Xiong, H. M.; Chen, W. Y.; Lee, K. M.; Van Horn, R. M.; Quirk, R. P.; Lotz, B.; Thomas, E. L.; Shi, A. C.; Cheng, S. Z. D. *Macromolecules* **2006**, *39*, 641.
(34) Quirk, R. P.; Kim, J.; Kausch, C.; Chun, M. S. *Polym. Int.* **1996**, *39*, 3.
(35) Lotz, B.; Kovacs, A. J.; Bassett, G. A.; Keller, A. *Kolloid Z. Z. Polym.* **1966**, *209*, 115.
(36) Lotz, B.; Kovacs, A. J. *Kolloid Z. Z. Polym.* **1966**, *209*, 97.
(37) Hsiao, M. S.; Zheng, J. X.; Leng, S. W.; Van Horn, R. M.; Quirk, R. P.; Thomas, E. L.; Chen, H. L.; Hsiao, B. S.; Rong, L. X.; Lotz, B.; Cheng, S. Z. D. *Macromolecules* **2008**, *41*, 8114.
(38) Hsiao, M. S.; Chen, W. Y.; Zheng, J. X.; Van Horn, R. M.; Quirk, R. P.; Ivanov, D. A.; Thomas, E. L.; Lotz, B.; Cheng, S. Z. D. *Macromolecules* **2008**, *41*, 4794.
(39) Hsiao, M. S.; Zheng, J. X.; Horn, R. M. V.; Quirk, R. P.; Thomas, E. L.; Chen, H. L.; Lotz, B.; Cheng, S. Z. D. *Macromolecules* **2009**, *42*, 8343.
(40) Mai, S. M.; Booth, C.; Nace, V. M. *Eur. Polym. J.* **1997**, *33*, 991.
(41) Lichtenthaler, R. N.; Liu, D. D.; Prausnitz, J. M. *Macromolecules* **1978**, *11*, 192.
(42) Zheng, X. The Study of Onsets of Tethered Chain Overcrowding and Highly Stretched Brush Regime via Crystalline-amorphous Diblock Copolymers. Ph.D. Dissertation, The University of Akron, Akron, Aug 2005.
(43) Booth, C.; Orme, R. *Polymer* **1970**, *11*, 626.
(44) Buyuktanir, E. A.; Kucukyavuz, Z. *J. Polym. Sci., Part B: Polym. Phys.* **2000**, *38*, 2678.
(45) Sakurada, I.; Kaji, K.; Nakamae, K.; Wadano, S. *Chem. High Polym.* **1969**, *26*, 556.
(46) Lovett, D. R. *Tensor Properties of Crystals*, 2nd ed.; Institute of Physics Pub.: Philadelphia, 1999.
(47) Wunderlich, B. *Thermal Analysis*; Academic Press: Boston, 1990.